

Inorganic Synthesis for the Stabilization of Nanoparticles: Application to Cu/Al₂O₃ Nanocomposite Materials

Yu Xing,[†] Zhenxin Liu,[†] and Steven L. Suib^{*,†,‡}

Department of Chemistry and Department of Chemical, Materials & Biomolecular Engineering,
University of Connecticut, Storrs, Connecticut 06269-3060

Received May 9, 2007. Revised Manuscript Received July 9, 2007

A series of copper/aluminum nanocomposites with different mixing homogeneities and different texture features were prepared via various inorganic synthesis methods including coprecipitation, gelation, and stepwise thermal modification. Nitrogen sorption measurements and X-ray diffraction were used for textural and structural analysis, respectively. Solid–solid reaction analysis and differential scanning calorimetry (DSC) analysis were developed for the determination of the mixing homogeneities of copper-based nanocomposite materials. A sintering experiment at 250–600 °C for 350 h under methanol-steam reforming conditions was carried out to compare the stability of supported Cu⁰ nanoparticles. Although a large initial size of supported nanoparticles is not favorable, those supported nanoparticles with a small initial size cannot ensure good thermal stability. The mixing homogeneities of CuO/Al₂O₃ mixed metal oxide (MMO) nanocomposites significantly affected the thermal stability of their reduced Cu⁰ crystallites. Besides homogeneity control, creation of narrow distributions of pore sizes with small major pore diameters (e.g., around 3.5 nm) can also be used for the stabilization of supported Cu⁰ nanoparticles. We found that mixing homogeneity of a nanocomposite is likely the major factor in the stabilization of nanoparticles, whereas a narrow distribution of pore sizes might confine the growth of nanoparticles, possibly via space limitations. Field-emission scanning electron microscopy (FESEM), high-resolution transmission electron microscopy (HRTEM), and convergent beam electron diffraction (CBED) were used for the observation or structure determination of the copper/aluminum nanocomposites. This paper also provides information on the deactivation of copper catalysts via thermal sintering under methanol-steam reforming conditions.

1. Introduction

The thermal stability of metal or metal oxide nanoparticles is generally improved by dispersing them on ceramic supports like alumina and silica.¹ The small metal or metal oxide crystallites often are anchored to them by van der Waals forces or chemical bonds, thus avoiding particle migration and subsequent coalescence of particles.^{1,2}

When two or more phases are mixed together via physical or chemical methods to make a nanocomposite, a combination of properties may be obtained, which are not available in any of the individual components.³ Homogeneity of a nanoparticle mixture, representing the quality of nanoparticle mixing and defined here as the degree of mixing (or homogenization) of the nanoparticles of different phases, is important for the performance of structural materials, coatings, catalysts, and advanced energetic, electronic, photonic, and magnetic materials.³

The degree of mixing has been determined by analyzing images of particle arrays using microscopy, photography, and/or video tools. However, for nanoparticle mixtures,

obtaining a reliable assessment of particle positions in an array and distinguishing between the different species are very difficult.³ In this work, copper-containing nanocomposites were studied as examples of mixed metal oxide (MMO), metal/support, and decomposable nanocomposite materials.

The homogeneous deposition–precipitation (HDP) method with the use of urea at 90 °C, which does not produce gels but produces precipitates, has been developed by Geus et al. for the preparation of highly loaded and highly dispersed oxide-supported metal catalysts.⁴ A novel urea-gelation/thermal-modification method, which produces copper/aluminum gels after gelation and is different from the HDP method of ref 4, was used in this paper to provide copper/aluminum nanocomposites with narrow distributions of pore sizes and small major pore sizes (e.g., around 3.5 nm), for the stabilization of Cu⁰ nanoparticles.

Herein, we present the preparation of copper/aluminum nanocomposites with different texture features and different homogeneities using various inorganic synthesis methods, the determination of mixing homogeneity of nanocomposites via solid–solid reaction analysis and differential scanning calorimetry (DSC) analysis, the “hereditary” character of nanocomposites in homogeneity, and the stabilization of

* Corresponding author. E-mail: steven.suib@uconn.edu.

[†] Department of Chemistry, University of Connecticut.

[‡] Department of Chemical, Materials & Biomolecular Engineering, University of Connecticut.

(1) Moulijn, J. A.; van Diepen, A. E.; Kapteijn, F. *Appl. Catal., A* **2001**, 3–16.

(2) Butt, J. B.; Peterson, E. E. *Activation, Deactivation, and Poisoning of Catalysts*; Academic Press: San Diego, 1988; p 225.

(3) Wei, D.; Dave, R.; Pfeffer, R. *J. Nanopart. Res.* **2002**, 21–41.

(4) (a) Hermans, L. A. M.; Geus, J. W. *Stud. Surf. Sci. Catal.* **1979**, 3, 113–130. (b) Bezemer, G. L.; Radstake, P. B.; Koot, V.; van Dillen, A. J.; Geus, J. W.; de Jong, K. P. *J. Catal.* **2006**, 237, 291–302.

Table 1. Nomenclature of Uncalcined Xerogel/Precipitates

denomination of xerogel/precipitates ^a	CuO/Al ₂ O ₃ ratio ^b	
	nominal ratio (wt %)	actual ratio (wt %)
C100-NaHCO ₃	100/0	100.0/0.0
A100-NaHCO ₃	0/100	0.0/100.0
CA50-NaHCO ₃	50/50	49.8/50.2
CA50-Na ₂ CO ₃	50/50	51.4/48.6
CA50-(NH ₄) ₂ CO ₃	50/50	48.9/51.1
CA50-3.0Urea	50/50	53.2/46.8
CA50-1.0Urea	50/50	52.4/47.6
CA30-(NH ₄) ₂ CO ₃	30/70	27.2/72.8

^a C, copper; A, aluminum; 50, nominal ratio for prior element; Urea, precipitant; 3.0, times of stoichiometric requirement of the precipitant used for synthesis. Others are defined similarly. ^b Elemental composition.

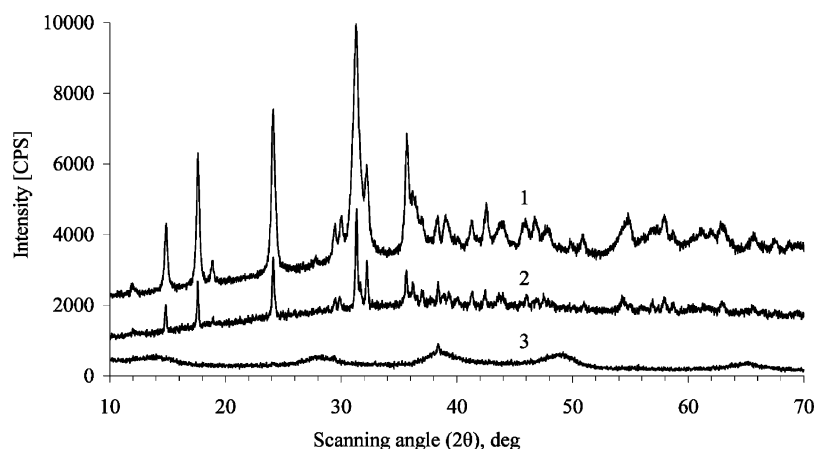


Figure 1. X-ray diffraction (XRD) patterns of uncalcined precipitates. (1) C100-NaHCO₃, (2) CA50-NaHCO₃, (3) A100-NaHCO₃.

supported nanoparticles via the control of mixing homogeneity and the tuning of pore size distribution. The method of determining mixing homogeneity via solid–solid reaction analysis has potential applications for mixed oxide materials/catalysts that solid–solid reactions, e.g., the formation of AB₂O₄ spinels or ABO₃ perovskites, can occur under appropriate temperature.

In light of the importance of copper-based catalysts in methanol synthesis, steam reforming, and decomposition reactions, surprisingly, there is not a wealth of information available on the deactivation of copper catalysts in these reactions.⁵ In contrast, the literature on the deactivation of, for example, platinum and nickel catalysts is much more extensive than the literature on the deactivation of copper catalysts.⁵ This paper also provides information on the deactivation of copper catalysts via thermal sintering under methanol-steam reforming conditions. In summary, this paper focuses on the materials science (e.g., thermal stability) of copper-based nanocomposites. Catalytic properties of these materials will be covered elsewhere.

2. Experimental Section

2.1. Synthesis. The sources of Al and Cu were Al(NO₃)₃·9H₂O and Cu(NO₃)₂·3H₂O, respectively (all from Strem Chemicals, Inc.), whereas the dosages were all determined on the basis of the nominal ratios in Table 1. Xerogel CA50-3.0Urea and precipitate CA50-1.0Urea were gelated and precipitated, respectively, at 100 °C under vigorous stirring by reacting 3.0 and 1.0 times the stoichiometric requirement of the precipitant urea with the solutions of Al and Cu sources. The former was dried at 180 °C and the latter at

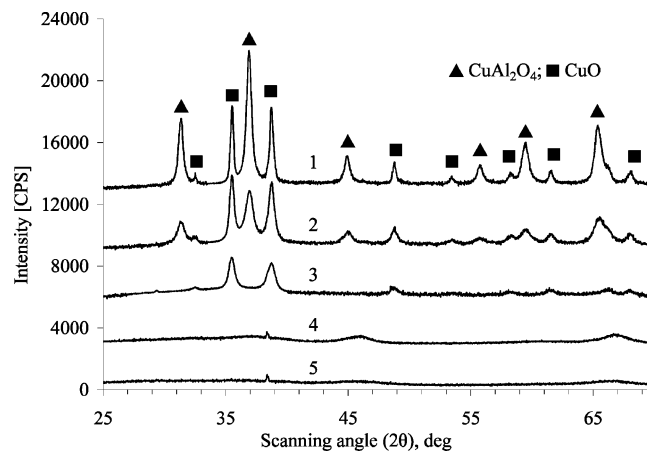


Figure 2. XRD patterns of calcined precipitates. (1) CA50-NaHCO₃, calcined at 900 °C for 3 h, (2) CA50-NaHCO₃, 700 °C/3 h, (3) CA50-NaHCO₃, 400 °C/3 h, (4) A100-NaHCO₃, 700 °C/3 h, (5) A100-NaHCO₃, 400 °C/3 h.

100 °C, without filtration or washing for both. Others were all precipitates, prepared with 1.05 times the stoichiometric requirements of precipitants at 50 °C under vigorous stirring by conventional coprecipitation methods, filtered after 1 h digestion, washed by water, and dried at 100 °C. Air was the atmosphere used in drying and calcining. The 250–600 and 250–800 °C sintering experiments were conducted in helium by loading powders in quartz boats in a tubular furnace, fueled with a CH₃OH/H₂O mixture at a methanol-based weight hourly space velocity of 0.36 h⁻¹. At each temperature stage, samples were quickly cooled to room temperature, after 2 and 50 h (250–600 °C sintering experiment), or after 5 and 50 h (250–800 °C sintering experiment), for XRD scans.

2.2. Characterization. The elemental compositions of the products were determined by an IRIS ICP-OES. Crystalline phases were identified by powder X-ray diffraction using a Scintag XDS-

Table 2. Formation of CuAl_2O_4 Phase in Calcined Materials

materials before calcination	calcination process	$L_{\text{CuO}(-111)}^a$ (nm)	$I(\text{CuAl}_2\text{O}_4)/I(\text{CuO})^b$
CA50- $(\text{NH}_4)_2\text{CO}_3$	700 °C/3 h	11.9	5.01
CA50- NaHCO_3	900 °C/3 h	29.5	1.59
CA50- NaHCO_3	700 °C/3 h	17.5	0.72
CA50-3.0Urea	700 °C/3 h	11.8	0.33
CA50-1.0Urea	700 °C/3 h	9.2	0.14
CA50- Na_2CO_3	700 °C/3 h	16.6	0.10
CA50-mixture ^c	700 °C/3 h	23.2	0.05
C100- NaHCO_3	700 °C/3 h	54.6	N/A

^a Average CuO crystallite size in the direction perpendicular to the (-111) reflecting planes. Other similar terms follow this definition. ^b XRD peak intensity ratio of CuAl_2O_4 (311) to CuO (-111) . I , the intensity of a XRD peak determined by background subtraction and curve fitting. ^c Powder mixture of C100- NaHCO_3 and A100- NaHCO_3 were ground together for 30 min, mixed in water in a Vortex mixer at 500 rpm for 2 h, and then centrifuged and dried at 100 °C.

2000 diffractometer with Cu $K\alpha$ radiation. Volume-weighted average crystallite sizes were determined by X-ray diffraction line broadening analysis (LBA), where data of integral line breadth were employed using a Scherrer constant of 1.0.⁶ A Micromeritics ASAP 2010 surface area system was used for nitrogen sorption measurements. Desorption branches of isotherm plots were used for BJH pore distribution analysis. Thermal analyses were carried out using a DSC 2920 differential scanning calorimeter and a Perkin-Elmer TGA-7 in nitrogen with ramps of 10 °C/min. Field-emission scanning electron microscopy (FESEM) studies were carried out using a Zeiss DSM 982 Gemini FESEM with a Schottky emitter operated at 10 kV and a beam current of about 1 μA . High-resolution transmission electron microscopy (HRTEM) combined with convergent beam electron diffraction (CBED) was employed for structure analysis using a JEOL 2010 FastEM with an accelerating voltage of 200 kV.

3. Results and Discussion

3.1. Synthesis and Characterization. A group of decomposable materials were prepared by coprecipitation and gelation methods. As listed in Table 1, all actual compositions are close to their nominal ones. XRD patterns in Figure 1 show that the uncalcined C100- NaHCO_3 is a crystalline malachite ($\text{Cu}_2\text{CO}_3(\text{OH})_2$) phase. XRD and thermogravimetric analyses show that the uncalcined A100- NaHCO_3 is an X-ray amorphous $\text{Al}(\text{OH})_3$ phase. The uncalcined CA50- NaHCO_3 is a nanocomposite composed of mixed $\text{Cu}_2\text{CO}_3(\text{OH})_2$ and $\text{Al}(\text{OH})_3$ nanoparticles.

As shown in Figure 2, the $\text{Al}(\text{OH})_3$ phase (A100- NaHCO_3) decomposed into an X-ray amorphous Al_2O_3 phase after calcination at 400 or 700 °C. After calcination at 400 °C, CA50- NaHCO_3 became a nanocomposite of mixed CuO and Al_2O_3 phases. After calcination at 700 °C, CA50- NaHCO_3 became a nanocomposite of mixed CuO, Al_2O_3 , and CuAl_2O_4 phases. These data suggest that the CuAl_2O_4 phase is the product of the solid–solid reaction between CuO and Al_2O_3 phases. This is consistent with that found in literature.⁷ Other copper/aluminum xerogel/precipitates have similar thermal decomposition behavior: CuO and Al_2O_3 phases were produced at a low temperature, whereas a CuAl_2O_4 phase was formed at 700 °C. The rate of a solid–solid reaction depends on the particle size of the reactants, the degree of

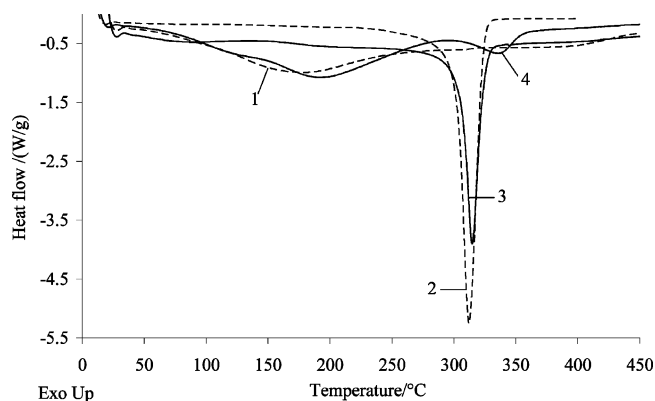


Figure 3. Differential scanning calorimetry (DSC) curves for uncalcined precipitates/xerogels. (1) A100- NaHCO_3 , (2) C100- NaHCO_3 , (3) CA50-mixture, (4) CA50- NaHCO_3 .

homogenization achieved on mixing, and the intimacy of contact between the grains, as well as the temperature.⁸ The sizes of CuO crystallites and Al_2O_3 particles in different samples are in narrow ranges, and therefore, the particle size effect on this solid–solid reaction is considered to be negligible. After calcination at 900 °C, more CuAl_2O_4 phase was produced, as revealed by the obviously higher ratio of peak intensities of CuAl_2O_4 (311) to CuO (-111) . This indicates that this solid–solid reaction at 700 °C was less affected by atomic/particle migration than that at 900 °C. Thus, it appears that CuAl_2O_4 formation during calcination at 700 °C can be used to determine the homogeneities of CuO/ Al_2O_3 MMO nanocomposites. The results are listed in Table 2. An order of the homogeneities of CuO/ Al_2O_3 nanocomposites can be obtained (using the nomenclature of their uncalcined precursors): CA50- $(\text{NH}_4)_2\text{CO}_3$ > CA50- NaHCO_3 > CA50-3.0Urea > CA50-1.0Urea > CA50- Na_2CO_3 > CA50-mixture. After calcination at 700 °C, the average size (23.2 nm) of the CuO crystallites in the CA50-mixture was significantly smaller than the size (54.6 nm) in C100- NaHCO_3 . This suggests that compared with the pure malachite phase in C100- NaHCO_3 , mechanical mixing of malachite phase with $\text{Al}(\text{OH})_3$ phase did improve the thermal stability, herein the resistance to sintering, of the produced CuO nanoparticles.

Precipitate CA50- NaHCO_3 is structurally composed of mixed nanoparticles of C100- NaHCO_3 and A100- NaHCO_3 . This coincidence occurred only when NaHCO_3 was used as

(6) Bergeret, G.; Gallezot, P. In *Handbook of Heterogeneous Catalysis*, Vol. 2; Ertl, G., Knözinger, H., Weitkamp, J., Eds.; VCH: Weinheim, Germany, 1997; pp. 446–450.

(7) (a) Luo, M.-F.; Fang, P.; He, M.; Xie, Y.-L. *J. Mol. Catal. A: Chem.* **2005**, 243–248. (b) Shaheen, W. M. *Thermochim. Acta* **2002**, 105–116.

(8) West, A. R. *Solid State Chemistry and Its Applications*; Wiley: Chichester, U.K., 1984; p 16.

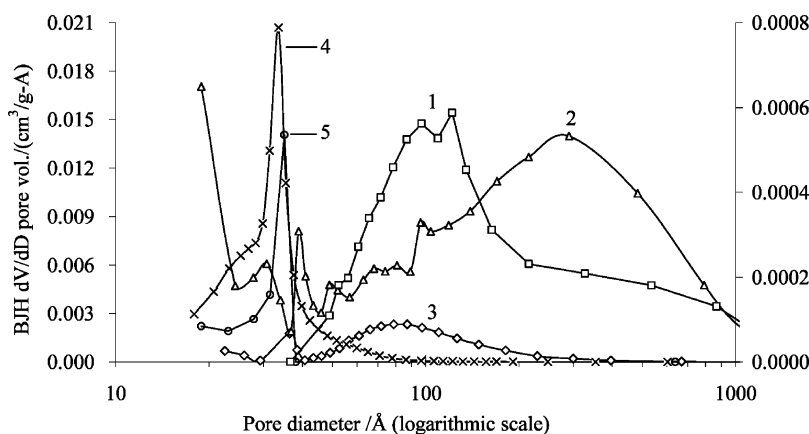


Figure 4. BJH pore size distribution of calcined nanocomposites. (1) CA50-(NH₄)₂CO₃-700°C, (2) CA50-NaHCO₃-400°C, (3) CA50-Na₂CO₃-400°C, (4) CA50-3.0Urea-400°C, (5) CA50-1.0Urea-400°C 1 and 2 follow the scale of the right ordinate axis and 3–5 follow the scale of the left ordinate axis.

Table 3. Nomenclature and Physical Properties of Nanocomposites for the 250–600 °C Sintering Experiments

denomination of calcined xerogel/precipitates	calcn. process	L_{CuO} (nm)	pore diameter (nm) ^a	SA (m ² /g) ^b	
				before MSR	after MSR
CA50-(NH ₄) ₂ CO ₃ -700°C	700 °C/3 h	11.9	22.4	47	74
CA50-NaHCO ₃ -400°C	400 °C/3 h	13.2	21.6	70	61
CA50-Na ₂ CO ₃ -400°C	400 °C/3 h	6.5	10.3	122	60
CA50-3.0Urea-400°C	250 °C/2 h, 400 °C/3 h	7.6	4.2	217	94
CA50-1.0Urea-400°C	250 °C/2 h, 400 °C/3 h	8.5	3.8	150	87

^a Average pore diameter (4V/A by BET). ^b BET specific surface area.

the precipitant. A mechanical mixture of C100-NaHCO₃ and A100-NaHCO₃ powders, named CA50-mixture, was made to have the same composition as CA50-NaHCO₃. In the temperature range below 400 °C, malachite and Al(OH)₃ phases simply decompose to form CuO and Al₂O₃, respectively, and do not react with each other. DSC was applied in both physical changes such as melting and chemical reactions such as decomposition.⁹ As shown in Figure 3, the DSC curve for the amorphous Al(OH)₃ phase (A100-NaHCO₃) contains a short and broad major peak at 179 °C, whereas the malachite phase DSC curve has an intense and sharp decomposition peak at 312 °C. Comparing the DSC curve with that of C100-NaHCO₃, the peaks for the malachite phase in the CA50-mixture and CA50-NaHCO₃ shifted to 315 and 336 °C, respectively. The peaks for the malachite phase in the CA50-mixture and C100-NaHCO₃ are intense and sharp, whereas that in CA50-NaHCO₃ is short and broad. The malachite nanoparticles in C100-NaHCO₃ are aggregated because nothing segregated them, whereas those in CA50-NaHCO₃ are dispersed because the Al(OH)₃ phase segregated them. Therefore the location and shape of the peak for the malachite phase can be used to determine the homogeneity of malachite/Al(OH)₃ nanocomposites. Curve 3 is more similar to curve 2 than curve 4. This indicates that the malachite nanoparticles in CA50-NaHCO₃ are dispersed much better than in the CA50-mixture. Therefore, the order of the homogeneities of malachite/Al(OH)₃ nanocomposites can be made: CA50-NaHCO₃ > CA50-mixture. Combining with the order for the homogeneities of CuO/Al₂O₃ nanocomposites, a “hereditary” character was revealed: the homogeneity of a decomposable copper/aluminum nanocomposite dominated the homogeneity of its decomposed product.

3.2. Stability of Copper Nanoparticles. Sintering is a gradual increase in the average size of crystallites or growth of the primary particles in a material/catalyst at temperatures below the melting point of the crystallites or particles. Sintering leads to a decrease in surface area (SA).¹⁰ Lifetime of materials and catalysts may be significantly affected by their resistance to sintering. Supported Cu⁰ nanocomposites may be useful as electronically conducting materials (e.g., in solid oxide fuel cells) or industrial catalysts.^{11,12} Table 3 and Figure 4 show the texture features of the calcined copper/aluminum nanocomposites prepared for the 250–600 °C sintering experiment under methanol-steam reforming (MSR) conditions, from which reducing gases such as H₂ will be produced over supported copper catalysts. The CA50-3.0Urea-400°C and CA50-1.0Urea-400°C samples have narrow distributions of pore sizes with a major pore diameter at 3.35 and 3.50 nm, respectively, whereas the pores of the other three are all widely distributed with much larger average pore diameters. Stepwise thermal modification at 250 and 400 °C was used to enhance the narrowing of pore sizes of CA50-3.0Urea-400°C and CA50-1.0Urea-400°C. The calcination of a small quantity of urea-containing Cu/Al composite materials in a muffle furnace was safe, but special precautions regarding hazards (e.g., temperature runaway) might have to be taken during the heat-treatment

- (9) Haines, P. J.; Wilburn, F. W. *Thermal Methods of Analysis*; Blackie Academic & Professional: Glasgow, Scotland, 1995; p 78.
- (10) Falconer, J. L. In *Catalysis: Science and Technology*; Anderson, J. R., Boudart, M., Eds.; Springer-Verlag: Berlin, 1996; Vol. 10, p 202.
- (11) (a) Park, S.; Vohs, J. M.; Gorte, R. J. *Nature* **2000**, 265–267. (b) Boder, M.; Dittmeyer, R. *J. Power Sources* **2006**, 13–22.
- (12) (a) Frank, B.; Jentoft, F. C.; Soerijanto, H.; Kroehnert, J.; Schloegl, R.; Schomaecker, R. *J. Catal.* **2007**, 177–192; (b) Twigg, M. V. *Catalyst Handbook*; Manson Publishing: London, 1996; p 455–468.

Table 4. Nomenclature of Nanocomposites for the 250–800 °C Sintering Experiment

denomination of calcined precipitates	calcn. of precipitates	L_{CuO} (nm)	$I(\text{CuAl}_2\text{O}_4)/I(\text{CuO})$
CA30-(NH_4) $_2\text{CO}_3$ -600°C	400 °C/3 h, 500 °C/1 h, 600 °C/2 h	35.0	0.36
CA30-(NH_4) $_2\text{CO}_3$ -750°C	750 °C/3 h	N/A ^a	∞
C100-NaHCO $_3$ -400°C	400 °C/3 h	23.4	N/A

^a No CuO phase. $L_{\text{CuAl}_2\text{O}_4(311)} = 4.7$ nm.

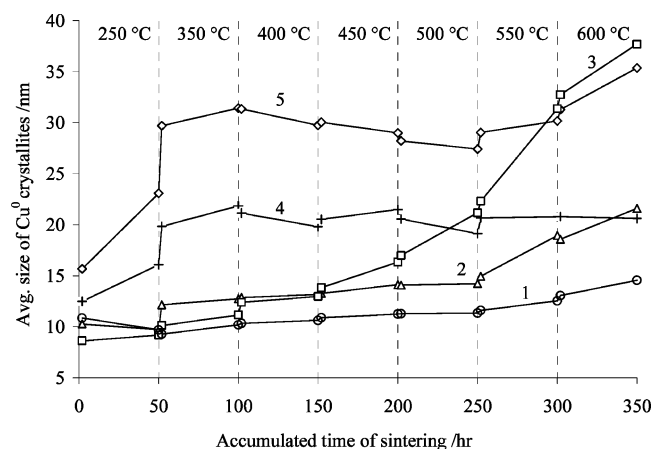


Figure 5. Average crystallite sizes $L_{\text{Cu}(111)}$ of reduced nanocomposites during the 250–600 °C sintering experiments. (1) CA50-(NH_4) $_2\text{CO}_3$ -700°C, (2) CA50-NaHCO $_3$ -400°C, (3) CA50-Na $_2\text{CO}_3$ -400°C, (4) CA50-3.0Urea-400°C, (5) CA50-1.0Urea-400°C.

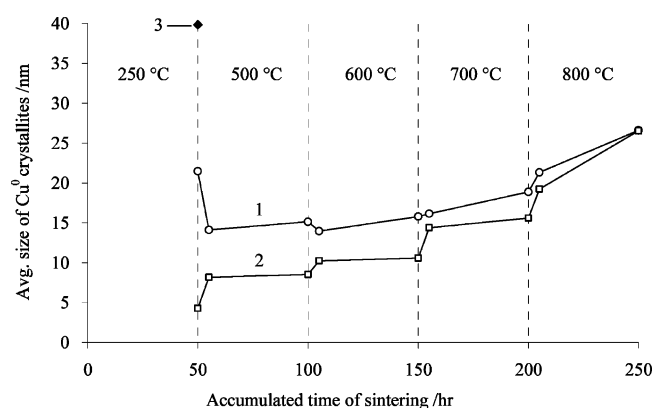


Figure 6. Average crystallite sizes $L_{\text{Cu}(111)}$ of reduced materials during the 250–800 °C sintering experiment. (1) CA30-(NH_4) $_2\text{CO}_3$ -600°C, (2) CA30-(NH_4) $_2\text{CO}_3$ -750°C, (3) C100-NaHCO $_3$ -400°C.

of a large quantity of urea-containing Cu/Al composite materials.

X-ray diffraction line broadening analysis (LBA) is widely used for characterizing the average size of crystallites such as supported metal crystallites and is well-suited for the study of sintering.⁶ The LBA data of this sintering experiment are shown in Figure 5. All CuO phases were reduced to Cu⁰ at 250 °C, whereas the Cu⁰ phase was gradually produced during the reduction of the CuAl $_2$ O $_4$ phase in CA50-(NH_4) $_2$ -CO $_3$ -700°C and became a dominant crystalline phase by the end of the 350 °C stage. The five sintering curves in Figure 5 can be divided into two distinct categories: two with narrowly distributed pore sizes that both have a “sintering stop zone” (350–600 °C for CA50-3.0Urea-400°C, 350–500 °C for CA50-1.0Urea-400°C) where the average sizes of Cu⁰ crystallites stopped increasing; whereas the average sizes of Cu⁰ crystallites of the other three, which

have widely distributed pore sizes, all have an increasing trend, fast or slow, during this sintering experiment. These results suggest that narrowly distributed pore structures can prevent the supported Cu⁰ crystallites from further growth over a wide temperature range, and suggest that the copper/aluminum nanocomposite with a better homogeneity may have a wider sintering stop zone. The reduced CA50-3.0Urea-400°C and CA50-1.0Urea-400°C show a rapid increase in Cu⁰ crystallite sizes below 350 °C, but the reasons are not yet fully understood.

Sintering of Cu⁰ crystallites in reduced CA50-3.0Urea-400°C and CA50-NaHCO $_3$ -400°C samples was much less severe than those in reduced CA50-1.0Urea-400°C and CA50-Na $_2$ CO $_3$ -400°C samples, respectively. These results suggest that the better the homogeneity of a CuO/Al $_2$ O $_3$ MMO, the less its reduced Cu⁰ crystallites sinter. For a nanocomposite with a certain composition, sintering of a component like Cu⁰ crystallites depends on how well it is dispersed by a refractory component like Al $_2$ O $_3$. The interaction between metal and oxide support is mainly due to van der Waals forces.² The larger the area of the “adhering” interface between Cu⁰ crystallites and the Al $_2$ O $_3$ phase, the better the Cu⁰ crystallites can be “anchored” on the surface of the Al $_2$ O $_3$ phase to minimize particle migration and thus increase the resistance to sintering. Therefore, the homogeneity of a Cu⁰/Al $_2$ O $_3$ nanocomposite can be deduced from its resistance to sintering. The “hereditary” character of the homogeneity of a nanocomposite may be further extended: the homogeneity of a CuO/Al $_2$ O $_3$ MMO nanocomposite dominates the homogeneity of its reduced product.

At the beginning of this sintering experiment, the reduced CA50-Na $_2$ CO $_3$ -400°C sample had the smallest average size (8.6 nm) of Cu⁰ crystallites. At the end of this sintering experiment, however, it had the largest average size (37.7 nm) of Cu⁰ crystallites. These data suggest that a small initial size of supported particles cannot ensure good thermal stability, which is significantly affected by the mixing homogeneity and pore size distribution of the material. The increase in the surface area of reduced CA50-(NH_4) $_2$ CO $_3$ -700°C, as shown in Table 3, is due to the released Al $_2$ O $_3$ during the reduction of the CuAl $_2$ O $_4$ phase. The smallest average size of Cu⁰ crystallites at the end of the 600 °C stage was achieved by reduced CA50-(NH_4) $_2$ CO $_3$ -700°C sample, the CuO/CuAl $_2$ O $_4$ nanocomposite with the best homogeneity, large average pore size, and broad pore size distribution. These data suggest that mixing homogeneity may have a more significant effect on the stabilization of nanoparticles than the pore size distribution. Mixing homogeneity of a nanocomposite is likely the major factor for the stabilization of nanoparticles, whereas a narrow distribution of pore sizes might confine the growth of nanoparticles, possibly via space limitations.

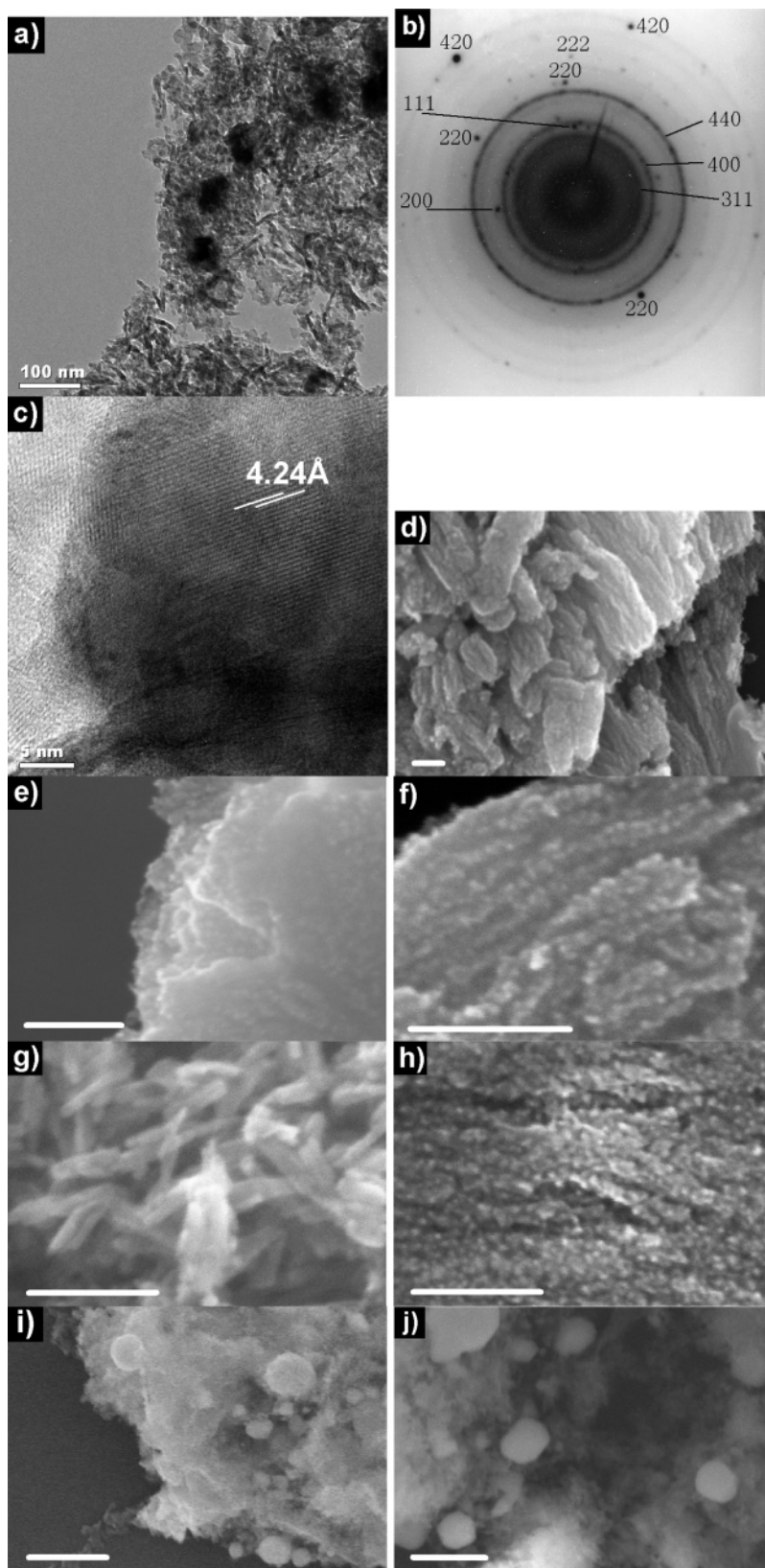


Figure 7. Electron microscopy studies of the nanocomposites after sintering experiments. (a–c) CA30-(NH₄)₂CO₃-750 °C after the 250–800 °C sintering experiment: (a) HRTEM image (scale bar, 100 nm), (b) electron diffraction pattern of a dark-colored substance, (c) lattice fringes of Cu–Al–O spinel phase (scale bar, 5 nm). (d–j) FESEM images of the samples after the 250–600 °C sintering experiment: (d–f) CA50-3.0Urea-400 °C (scale bars, 100 nm), (g) CA50-1.0Urea-400 °C (scale bar, 100 nm), (h) CA50-Na₂CO₃-400 °C (scale bar, 100 nm), (i) CA50-Na₂CO₃-400 °C (scale bar, 500 nm), (j) CA50-Na₂CO₃-400 °C (scale bar, 200 nm).

Table 4 shows the (CuO)/Al₂O₃/CuAl₂O₄ nanocomposites and CuO nanoparticles prepared for the 250–800 °C sintering experiment under MSR conditions. As shown in Figure

6, C100-NaHCO₃-400 °C was reduced to Cu⁰ and was significantly sintered at 250 °C. This explains why nonrefractory nanoparticles usually should be supported by refractory

phases. Curve 1 at 250 °C shows that very large CuO crystallites may produce unfavorably large Cu⁰ crystallites, and therefore should be avoided. At 250–700 °C, the Cu⁰ phase in curve 2 showed better thermal stability than that in curve 1. However, both curves 1 and 2 rise rapidly and converged at 800 °C, indicating that supported Cu⁰ materials should not be used at a temperature higher than 700 °C.

3.3. Electron Microscopy Studies. Because of poor electrical conductivity and contrast, individual Al₂O₃ nanoparticles are invisible to FESEM, which was used to observe the morphology of Al₂O₃ aggregates. Both FESEM and HRTEM can be used to observe individual Cu⁰ nanoparticles. The dark-colored substances in Figure 7a are mostly Cu⁰ single crystals that contribute to the diffraction spots of the electron diffraction pattern (Figure 7b), and some randomly oriented Cu–Al–O spinel polycrystals that give rise to the diffraction rings. Figure 7c shows the lattice fringes of a unit-cell-contracted Cu–Al–O spinel crystallite, in which the (111) *d*-spacing decreased to 0.424 nm. The light-colored substances in Figure 7a are Al₂O₃ nanoparticles, which seem cohesive but act as a carrier for dispersed Cu⁰ particles. Individual Al₂O₃ particles are round flakes with a diameter of about 8–10 nm and are randomly aggregated, whereas some are sintered as rodlike bars, observed also in reduced CA50-1.0Urea-400°C (Figure 7g), with a width of a single particle and a length of 40–65 nm. As shown in images d and e in Figure 7, the morphology of Al₂O₃ in reduced CA50-3.0Urea-400°C consists of aggregates of layered sheets, where Cu⁰ crystallites (Figure 7f) were anchored as dispersed arrays with crystallite sizes of around 8 nm. The average size of Cu⁰ crystallites of reduced CA50-Na₂CO₃-400°C is 37.7 nm, but the sizes of the Cu⁰ crystallites anchored on the Al₂O₃ sheet (Figure 7h) were only around 10 nm, which are much smaller than those giant Cu⁰ particles (images i and j in Figure 7) that stay unsupported in the “valleys” of the Al₂O₃ sheets. These images show how complicated a nanocomposite can be and how difficult it is to determine and compare the homogeneities of nanocomposites through high-resolution instruments, especially for these kinds of high concentration metal/support nanocomposites.

4. Conclusions

In summary, copper/aluminum nanocomposites with different texture features and different homogeneities

were prepared via different inorganic synthesis methods including gelation, coprecipitation, and stepwise thermal modification. Solid–solid reaction analysis and differential scanning calorimetry (DSC) analysis were developed for the determination of the mixing homogeneities of CuO/Al₂O₃ MMO and decomposable malachite/Al(OH)₃ nanocomposites, respectively. A “hereditary” character of the homogeneity of copper/aluminum nanocomposites was revealed: the homogeneity of a decomposable copper/aluminum nanocomposite (e.g., Cu₂CO₃(OH)₂/Al(OH)₃) may dominate the homogeneity of its decomposed product (e.g., CuO/Al₂O₃), and the latter continues to dominate the homogeneity of its reduced product (e.g., Cu⁰/Al₂O₃). These results clearly show the importance of the chemical synthesis of a nanocomposite and the homogeneity determination of as-synthesized nanocomposites. Although a large initial size of supported nanoparticles is not favorable, those supported nanoparticles with a small initial size cannot ensure good thermal stability. The mixing homogeneities of CuO/Al₂O₃ mixed metal oxide (MMO) nanocomposites significantly affect the thermal stability of their reduced Cu⁰ crystallites. Besides the homogeneity control, creation of narrow distributions of pore size with small major pore diameters (e.g., around 3.5 nm) can also be used for the stabilization of supported Cu⁰ nanoparticles.

Acknowledgment. We thank Dr. Francis Galasso for helpful suggestions, Dr. Jim Romanow and Dr. Sinue Gomez for helping to collect FESEM and HRTEM images, and the Institute of Materials Science at University of Connecticut for use of the microscopy facilities. This work was supported by the Geosciences and Biosciences Division of the Office of Basic Energy Sciences, Office of Science, U.S. Department of Energy.

Supporting Information Available: X-ray diffraction patterns collected during the 250–600 and the 250–800 °C sintering experiments under methanol-steam reforming conditions (PDF). This material is available free of charge via the Internet at <http://pubs.acs.org>.

CM0712570